

Investigation of the Richtmyer-Meshkov Instability with Stereolithographed Interfaces

Christian Mariani,¹ Marc Vandenboomgaerde,² Georges Jourdan,¹ Denis Souffland,² and Lazhar Houas^{1,*}

¹*Polytech'Marseille - Dpt Mécanique Énergétique - IUSTI/UMR CNRS 6595 Technopôle de Château Gombert, 5 rue Enrico Fermi, 13013 Marseille, France*

²*Commissariat à l'Énergie Atomique, CEA/DAM-Ile de France, Bruyères Le Châtel, 91297 Cedex, France*
(Received 16 February 2008; published 27 June 2008)

A novel method to set highly accurate initial conditions has been designed in the context of shock tube experiments for the Richtmyer-Meshkov instability study. Stereolithography has been used to design the membrane supports which initially materialize the gaseous interface. The visualizations of both heavy-light and light-heavy sinusoidal interfaces were carried out with laser sheet diagnostics. Experiments are in very good agreement with theory and simulations for the heavy-light case, but probably due to the membrane effects, quickly deviate from them in the light-heavy configuration.

DOI: [10.1103/PhysRevLett.100.254503](https://doi.org/10.1103/PhysRevLett.100.254503)

PACS numbers: 47.40.Nm, 47.20.Ma

The understanding of the mixing development process between two gases of different densities when their common interface undergoes acceleration is of great interest in many fields of research. Among them are the inertial confinement fusion (ICF), where it is necessary to control mixing in order to reach fusion, and on the other hand, the research on Scramjet where initial conditions are tested to enhance mix of fuel and oxidizer. Rayleigh [1] then Taylor [2] were the first to theoretically study the instability problem which occurs when a heavier fluid is suspended over a lighter fluid in constant gravity. Later, Richtmyer [3] then Meshkov [4] worked on the limit case of the Rayleigh-Taylor instability where the acceleration is impulsive and generated by a shock wave. In the case of the Richtmyer-Meshkov (RM) instability, the interface between the two gases is always unstable due to the vorticity production linked with the misalignment between the pressure and the density gradients when the shock wave passes through the interface. As a consequence, the interface perturbations grow and develop spikes and bubbles which can evolve into mushroom structures. These last digitations are later destabilized by shear flow (Kelvin-Helmoltz instability) that could lead to turbulent mixing.

Since its discovery, the RM instability has been studied in many theoretical, numerical, and experimental works. Pure hydrodynamics RM experiments are mainly realized in shock tubes. They constitute an effective means to study transition to turbulence and benchmarks for codes and models. The latter mainly deal with specific interfaces such as pure sinusoidal [3,5,6] and parabolic or triangular [7] shapes. Numerous papers [8–11] stress that the uncertainty about the initial conditions of the interface and the role of the membrane, which initially separates the gases in experiments, induce too much uncertainty in the use of experimental data to test numerical schemes. As a consequence, experiments that are more suited to both theoretical and numerical studies are needed: the initial conditions must be adjustable and well defined and the effects of extraneous items quantified. Unfortunately, in all known horizontal (membrane interface) or vertical (membraneless

but diffusive interface) shock tube experiments, the initial interfacial conditions are rarely accurately measured [4,11–17] but often backwards estimated. Thus, the aim of the present Letter is to investigate the growth of high accuracy known sinusoidal perturbations at a gaseous interface. To achieve the materialization of the initial interface, a thin nitrocellulosic membrane (0.5 μm thick) is deposited on a stereolithographed grid support, computer-aided designed and constructed with chosen shape and dimensions. This idea was originally initiated by M. Vandenboomgaerde (private communication, 2004). Stereolithography is a common technique in prototyping which allows to create 3D objects by solidification of a liquid resin at the location of a heating laser impact. We present here the first use of this technique to create accurate sinusoidal interfaces for RM experiments. Two grids have been built (mesh size: 1 cm \times 1 cm). Grid 1 perturbation represents a single period ($\lambda = 12$ cm) sinusoidal bump whereas Grid 2 perturbation has a two period sinusoidal shape ($\lambda = 8$ cm). Their shapes are described by the following functions: $\eta(y, 0) = \eta_0(1 - \cos ky)$ for $y \in [y_M, 200 - y_M]$ and $\eta(y, 0) = 0$ elsewhere. $\eta(y, t)$ is the amplitude of the perturbation, y the transverse dimension (in mm) of the shock tube, $k = 2\pi/\lambda$ the wave number, and where $\eta_0 = 6.89$ and 3.06 mm, $y_M = 40$ and 20 mm for Grids 1 and 2, respectively. We measured an accuracy better than 0.1 mm for the built grid dimensions. Let us note that we chose $k\eta_0 < 1$ in order to be amenable to linear and weakly nonlinear theories. Experiments are performed in a horizontal shock tube which is 7 m long, and 20×20 cm² square cross section. It is coupled with a high speed laser sheet device (1 frame/100 μs) which allows a 2D visualization of the interface. The imaging technique is based on the Mie scattering of a copper vapor laser light source (532 nm) by small smoke particles seeded in one of the two test gases (air). The experimental device is described in more details in the papers of Jourdan and Houas [13,18], where the accuracy about initial conditions was estimated with great difficulty. Incident shock wave Mach numbers are 1.15 and 1.4. Table I summarizes

TABLE I. Experimental parameters: A^* is the calculated post shock Atwood number, W_{is} (m/s) and W_{ts} (m/s) are the incident and the transmitted shock wave velocities. ΔU_{1D}^{exp} (m/s), η_0^* (mm), and λ (mm), represent the 1D experimental velocity jump of the interface, the post shock amplitude, and the wavelength of the initial perturbation, respectively.

Run	Grid	Gases	A^*	$W_{is} \pm 3\%$	$W_{ts} \pm 3\%$	$\Delta U_{1D}^{exp} \pm 3\%$	$\eta_0^* \pm 5\%$	$\lambda \pm 0.5\%$
113	2	air/SF ₆	+0.696	405	178	61	2.50	81
114	2	air/SF ₆	+0.665	408	185	66	2.50	81
120	2	air/SF ₆	+0.720	477	227	127	2.10	81
116	1	air/SF ₆	+0.696	405	178	61	5.50	122
117	1	air/SF ₆	+0.644	408	192	66	5.29	122
126	1	air/SF ₆	+0.721	480	217	131	4.89	122
121	2	air/He	-0.763	408	1111	137	1.91	82
123	2	air/He	-0.766	466	1180	221	1.5	82
124	1	air/He	-0.762	393	1084	105	6.00	123
125	1	air/He	-0.766	481	1207	269	3.21	122

the parameters of the present experiments. Figure 1 shows typical frames obtained for different gas configurations. On each picture, the perturbation amplitude is measured between the extreme points of the interface contour. One and two measurements are obtained for Grids 1 and 2, respectively, and the uncertainty is about $\pm 5\%$. The good quality of the frames allows to extract clear contours of the interface and points out different behaviors of the membrane particles: they quickly separate from the interface in the heavy-light case and remain stuck to it in the light-heavy case (white specks in Fig. 1). This has already been mentioned in an other experimental work [19]. Let us note that

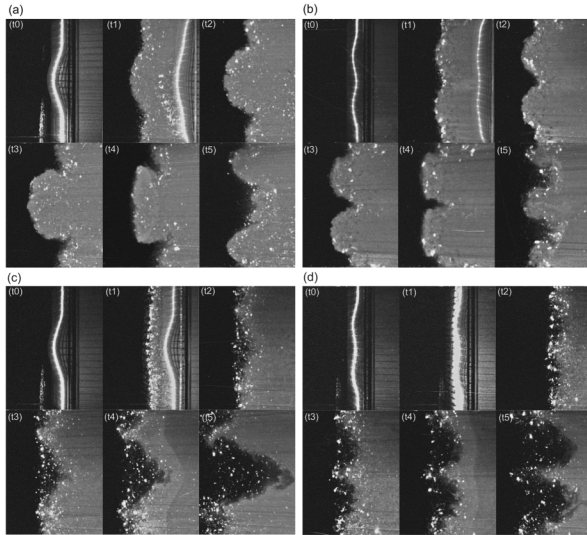


FIG. 1. Laser sheet pictures showing the interaction of a shock wave (moving from right to left) with a stereolithographed single mode interface for the light-heavy (air/SF₆) case with Grid 1 (a) and 2 (b) perturbations, and the heavy-light (air/He) case with Grid 1 (c) and 2 (d) perturbations. (a), (b), (c), and (d) are from runs 126, 120, 125, and 123, respectively, with a shock wave Mach number of about 1.4. Time between frames is approximately 300 and 800 μ s for the air/He and air/SF₆ experiments, and the compression of the interface by the reflected shock wave happens 1100 and 3200 μ s after the initial shock acceleration, respectively.

membrane particles experience higher drag in the SF₆ than in the He, and that their motion will be more slowed in the SF₆. Furthermore, the heavy-light interface reverses after the shock passage, and the near-interface velocity field favors particle motion away from the interface. These two mechanisms may explain the different behaviors of membrane particles in SF₆ and He. Figure 2 presents the time evolution of the amplitude $\eta(y, t)$ of the experiments described in Table I, compared with different models [5,12,20]. Amplitude and time are made dimensionless by scaling with k and $\eta_0^* k \sigma$, respectively. $\eta_0^* \sigma$ is the theoretical linear growth rate [3] and η_0^* the post shock amplitude. The linear phase of the RM instability occurs for $\tau = \eta_0^* k \sigma t < 1$ and $k[\eta(y, \tau) - \eta_0^*] < 1$. Let us remark that theories do not take into account grid and membrane effects. Furthermore, results are plotted before the interaction of the reflected shock wave with the interface. In the heavy-light configuration, we can see that the growth rate is almost a constant whatever the initial interface and the incident shock wave strength are. The very good agreement between experimental data and linear theory for $\tau < 1$, and models [20] seems to indicate no membrane effect:

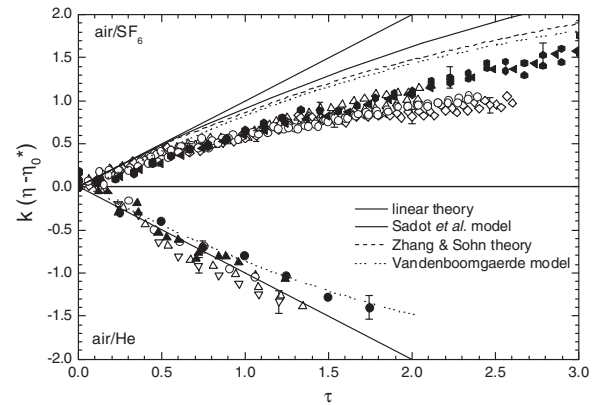


FIG. 2. Nondimensionalized time evolutions of the amplitude for light-heavy (up) and heavy-light (down) sinusoidal interfaces. Black and white symbols stand for experimental results at high and low Mach numbers, respectively.

this is consistent with the ejection of residual pieces of membrane away from the interface which is observed in this configuration. For the light-heavy gas interface, Fig. 2 shows that the growth rate is also independent of the sinusoidal dimensions of the interface and the incident shock wave strength, especially at the beginning of the growth ($\tau < 2$). However, in this case, comparisons with the nonlinear theory of Zhang and Sohn [5] and with the models of Sadot *et al.* [12] and Vandenboomgaerde [20], show that the experimental results are always lower than the theoretical predictions: the growth is reduced by 30% in comparison with the linear theory at $\tau = 1$. The discrepancy between experimental data and theories increases further for $\tau > 1$. As initial conditions can hardly be questioned, we explain this reduction, in the light-heavy configuration, by membrane effects on the interface dynamics: even without viscosity, an accelerated fluid induces a force $\vec{F} = \rho \frac{V_0}{2} \frac{d\vec{U}}{dt}$ upon a 3D floating supposed spherical object (where ρ and U are the density and velocity of the fluid, and V_0 the volume of the object) and thus, a part of the kinetic energy of the fluid at the interface is diverted to the particle motion. Let us remark that as the strength of the incident shock wave increases, the discrepancy is slightly reduced. In order to characterize the deformation of the perturbations into spike and bubble structures, the contours

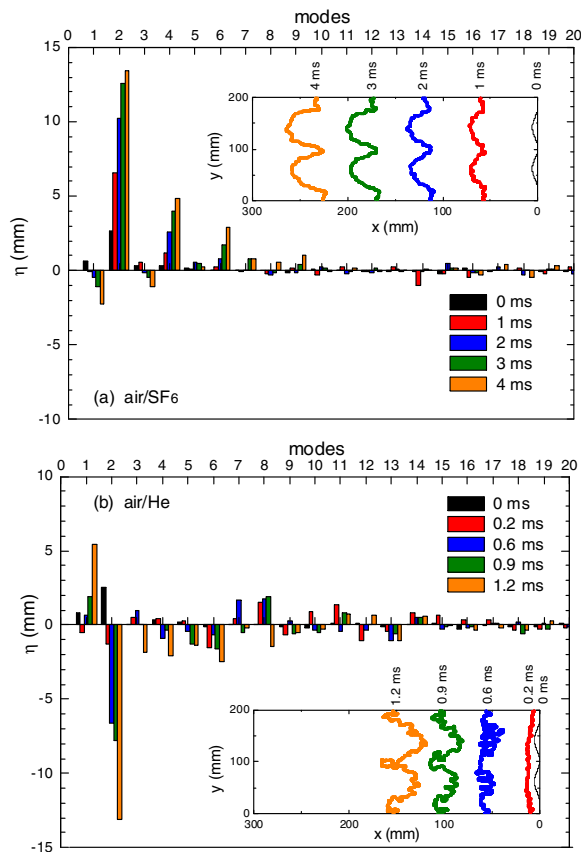


FIG. 3 (color online). Spectral analysis of the interface for the light-heavy run 113 (a) and heavy-light run 121 (b) at different times. Insets: extracted contours of the interface.

of the interfaces were extracted from each raw picture by an image processing and analyzed by a Fast Fourier Transform (FFT). Examples of this processing are presented for air/SF₆ and air/He interfaces in Fig. 3, at different times of their evolution. Each mode presents some noise which can be associated with bubble and spike distortions observed in Fig. 1. However, the modes introduced by the present grid technique have a characteristic length of 1 cm and should not strongly interact with the distant first harmonics. As the Fourier analysis is performed on a two period perturbation, the interface can be reconstructed as $\eta(y, \tau) = \sum_{n=1}^{\infty} \eta_n(\tau) \cos(ky/2)$. The amplitude of the fundamental mode and the two first harmonics are η_n for $n = 2, 4, \text{ and } 6$, respectively. Their time evolutions are plotted in Fig. 4 and compared with simulations [21] and the Vandenboomgaerde model [20]. Previous conclusions about perturbation growth are confirmed by FFT analysis: in the heavy-light configuration, the time evolutions of the fundamental mode, first and second harmonics are in very good agreement with numerical and theoretical results. This indicates that both grid, membrane, and associated modes have no effect on the studied wavelength. On the other hand, for the light-heavy case, a growth reduction is identified for the first two modes which increases with time. The relative discrepancies $\Delta\eta = (\eta_{\text{exp}} - \eta_{\text{sim}})/\eta_{\text{sim}}$ between experimental and numerical amplitudes are -20% , -29% , and -33% for the fundamental mode and -20% , -29% , and -30% for the first harmonics at $\tau = 1.5, 2, \text{ and } 2.5$, respectively. The increase of $\Delta\eta$ can be explained by continuous influence of the membrane pieces on the perturbation dynamics. This is consistent with the observation of the membrane pieces staying in the vicinity of the interface in the light-heavy case [Figs. 1(a) and 1(b)]. Further information is found in the analysis of the bubble and jet motion. Figure 5(a) shows the comparisons between bubble and jet locations for simulations, model, and experiments.

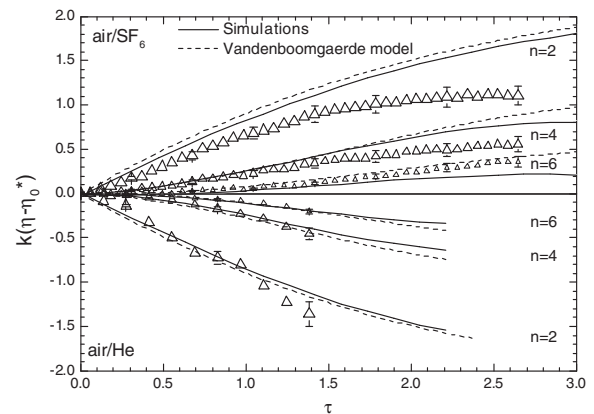


FIG. 4. Nondimensionalized time evolutions of the fundamental mode and its first and second harmonics amplitudes for the light-heavy run 113 (up) and heavy-light run 121 (down). Symbols stand for experimental results.

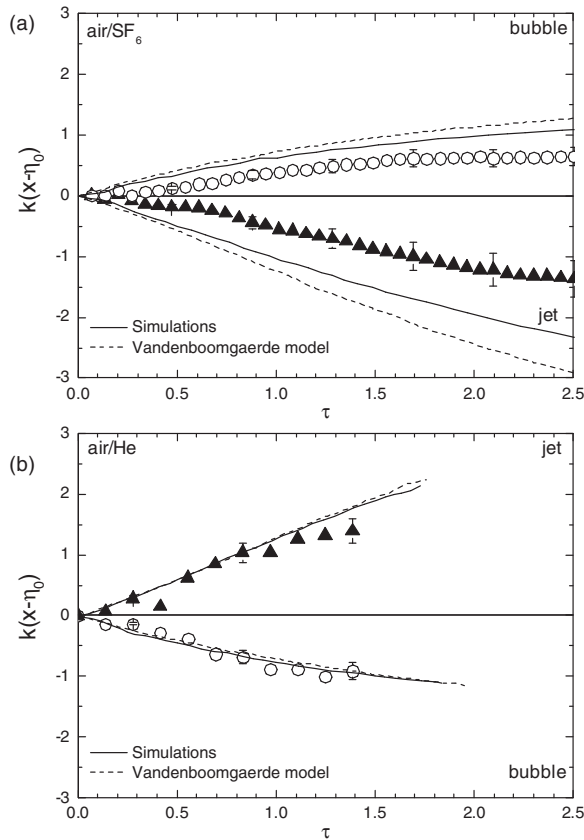


FIG. 5. Bubble and jet positions in a nondimensionalized system of axis for the light-heavy run 113 (a) and heavy-light run 121 (b). Symbols stand for experimental results.

The amplitude relative discrepancy is higher for the jet than for the bubble: $\Delta\eta = -38\%$ and -28% at $\tau = 2$, respectively. This statement is true whatever the moment. This strongly suggests more influence of the membrane particles on the jet dynamics than on the bubble one. This explanation is supported by pictures which show the motion of membrane pieces flowing from the bubble into the jet tips [Fig. 1(b) at t_1 , t_2 , and t_3]. On the other hand, for the heavy-light case, no influence of membrane is found as expected [Fig. 5(b)].

In summary, a novel method to produce an accurately-profiled initial interface has been developed to study the instability of a gaseous interface impulsively accelerated in a shock tube. The high accurate knowledge of the initial wavelength and amplitude of the interface coupled with high speed laser sheet visualization techniques enable fine comparisons with both theoretical and numerical works. Shock wave propagations from heavy to light as well as from light to heavy gas have been considered. For the former, we found a very good agreement between experimental, numerical, and theoretical growth rates, for zero-to-peak amplitude as well as for harmonics growth. This validates the accuracy which is obtained for initial conditions, and confirms that the membrane which is seen ejected away from the interface has no effect on the

perturbation dynamics. For the latter, experimental growth rates are always lower than numerical or theoretical ones. FFT, bubble, and jet velocity and image analysis can explain this reduction: the membrane pieces stay at the interface, and their flowing is imparted by a portion of the fluid kinetic energy which is normally devoted to the perturbation growth. This discrepancy has been quantitatively estimated. Such phenomena should be taken into account in the analysis of all shock tube experiments with membrane in the light-heavy cases for weak shock waves.

The authors would like to gratefully thank Professor Y. Zerega for running the FFT analysis and E. Brun for his help in image processing. This work is supported by CEA/DAM under Contract No. 4600124133/P6H29.

*lazhar.houas@polytech.univ-mrs.fr

- [1] L. Rayleigh, Proc. Lond. Math. Soc. **s1-14**, 170 (1882).
- [2] G. Taylor, Proc. R. Soc. A **201**, 192 (1950).
- [3] R. Richtmyer, Commun. Pure Appl. Math. **13**, 297 (1960).
- [4] E. Meshkov, Fluid Dyn. **4**, 101 (1972).
- [5] Q. Zhang and S. Sohn, Phys. Fluids **9**, 1106 (1997).
- [6] M. Vandenboomgaerde, S. Gauthier, and C. Mügler, Phys. Fluids **14**, 1111 (2002).
- [7] K. Mikaelian, Phys. Rev. Lett. **80**, 508 (1998).
- [8] D. Hill, C. Pantano, and D. Pullin, J. Fluid Mech. **557**, 29 (2006).
- [9] J. Grove, R. Holmes, D. Sharp, Y. Yang, and Q. Zhang, Phys. Rev. Lett. **71**, 3473 (1993).
- [10] K. Mikaelian, Phys. Rev. Lett. **71**, 2903 (1993).
- [11] P. Puranik, J. Oakley, M. Anderson, and R. Bonazza, Shock Waves **13**, 413 (2004).
- [12] O. Sadot, L. Erez, D. Oron, L. Levin, G. Erez, G. Ben-Dor, and D. Shvarts, Phys. Rev. Lett. **80**, 1654 (1998).
- [13] G. Jourdan and L. Houas, Phys. Rev. Lett. **95**, 204502 (2005).
- [14] D. Collins and J. Jacobs, J. Fluid Mech. **464**, 113 (2002).
- [15] B. Motl, J. Niederhaus, J. Oakley, D. Ranjan, M. Anderson, R. Bonazza, and J. Greenough, in *Proceedings of 10th International Workshop on the Physics of Compressible Turbulent Mixing*, edited by M. Legrand and M. Vandenboomgaerde (Paris, France, 2006).
- [16] D. Holder, A. Smith, C. Barton, and D. Youngs, Laser Part. Beams **21**, 411 (2003).
- [17] K. Prestridge, P. Vorobieff, P. Rightley, and R. Benjamin, Phys. Rev. Lett. **84**, 4353 (2000).
- [18] L. Houas, G. Jourdan, L. Schwaederle, R. Carrey, and F. Diaz, Shock Waves **12**, 431 (2003).
- [19] M. Brouillette and B. Sturtevant, Phys. Fluids **7**, 916 (1993).
- [20] M. Vandenboomgaerde, in *Proceedings of 9th International Workshop on the Physics of Compressible Turbulent Mixing*, edited by S. Dalziel (Cambridge, UK, 2004).
- [21] M. Boulet and J. Griffond, in *Proceedings of 10th International Workshop on the Physics of Compressible Turbulent Mixing*, edited by M. Legrand and M. Vandenboomgaerde (Paris, France, 2006).